Postprint of: Eremeyev VA. 2019 Strongly anisotropic surface elasticity and antiplane surface waves. Phil. Trans. R. Soc. A 378: 20190100. DOI: 10.1098/rsta.2019.0100

Strongly anisotropic surface elasticity and antiplane surface waves

V. A. Eremeyev[1,2]

[1]Faculty of Civil and Environmental Engineering, Gdańsk University of Technology, ul. Gabriela Narutowicza 11/12, 80-233 Gdańsk, Poland
[2]Research Institute for Mechanics, National Research Lobachevsky State University of Nizhni Novgorod, Nizhny Novgorod, Russia

VAE, 0000-0002-8128-3262

Research

Subject Areas:
materials science, mechanical engineering, applied mathematics

Keywords:
surface elasticity, anti-plane waves, nonlinear elasticity, metasurface, anisotropy

Author for correspondence:
Victor A. Eremeyev
e-mail: eremeyev.victor@gmail.com

Within the new model of surface elasticity, the propagation of anti-plane surface waves is discussed. For the proposed model, the surface strain energy depends on surface stretching and on changing of curvature along a preferred direction. From the continuum mechanics point of view, the model describes finite deformations of an elastic solid with an elastic membrane attached on its boundary reinforced by a family of aligned elastic long flexible beams. Physically, the model was motivated by deformations of surface coatings consisting of aligned bar-like elements as in the case of hyperbolic metasurfaces. Using the least action variational principle, we derive the dynamic boundary conditions. The linearized boundary-value problem is also presented. In order to demonstrate the peculiarities of the problem, the dispersion relations for surface anti-plane waves are analysed. We have shown that the bending stiffness changes essentially the dispersion relation and conditions of anti-plane surface wave propagation.

This article is part of the theme issue 'Modelling of dynamic phenomena and localization in structured media (part 2)'.

1. Introduction

Recent advances in design, modelling and manufacturing of light and sound-absorbing/reflecting, super-hydrophobic, superoleophobic and other microstructured coatings resulted in the appearance of a new class of metamaterials called metasurfaces, e.g. [1–7]. These coatings have rather complex geometry as they may consist of periodic or disordered lattice-like patterns formed on a surface. Continuum mechanics-based modelling of such surface-enhanced materials requires an adequate effective surface medium theory.

Among the models of surface elasticity, it is worth to mention the ones by Gurtin–Murdoch [8,9] and by Steigmann–Ogden [10,11], which are widely used at the micro- and nanoscale, e.g. [12–16]. In order to capture more complex material behaviour, some further extensions of surface/interfacial elasticity were proposed in [17–20].

The above-mentioned models of surface elasticity are based on the so-called direct approach, where we introduce additional constitutive relations defined at the surface or interface independently of the constitutive relations in the bulk. Another microstructural approach is based on the consideration of the thin solid surface/interfacial layer of finite thickness, e.g. [18,21–23], or of an interface consisting of various structural elements, such as point masses, springs, beams, etc., [24–31]. Within the microstructural approach, one has the possibility to analyse the microstructure in detail and its influence on a wave propagation along and across the surface/interface. It is worth also noting asymptotic methods for the analysis of boundary-layer type solutions in dynamics. In particular, a sort of near-surface membrane naturally arises even in the context of linear isotropic elasticity when dealing with the Rayleigh wave, e.g. [32] and references therein. Also, similar asymptotic phenomena occur in non-local elasticity when considering near-surface boundary layers, see [33], or for weakly non-local models such as strain-gradient media [34,35]. The comparison of the surface anti-plane wave propagation within the Gurtin–Murdoch surface elasticity was performed with Toupin–Mindlin strain-gradient elasticity [36] and in the case of lattice dynamics [37].

From the geometrical point of view, a metasurface can be described as a surface with a periodic array of holes, dots, discs, shells or cylinders [3–5,38,39], with a system of aligned bars [30,40–43], as a disordered foam-like coating [5,6,44], or as a lattice of complex resonating structural elements [1,2]. Here we restrict ourselves to the hyperbolic metasurfaces consisting of aligned bars or ribs [30,41–43]. Unlike material behaviour at the macrolevel, at the nanoscale there are interactions between these bars, which can be described using various models [45]. Instead we introduce here an averaged model where interfacial forces are described as membrane resultant stresses, but the bending stiffness of the bars is also taken into account. In the paper, we combine both direct and microstructural approaches. Considering coatings consisting of long thin ordered structured elements modelled as interacting elastic beams, we propose an averaged two-dimensional model of surface elasticity as in the direct approach. The proposed model describes finite deformations of an elastic solid with attached on its boundary or part an elastic membrane reinforced by aligned elastic beams.

The paper is organized as follows. In §2, we introduce the surface strain energy and derive the motion equations and the corresponding natural boundary conditions. To this end, we apply the least action principle. In §3, we present the linearized boundary-value problem for infinitesimal deformations. Finally, in §4, we consider surface anti-plane waves in an elastic half-space with the introduced surface strain energy.

rongly anisotropic surface elasticity

ving the surface elasticity approach, we introduce independently constitutive relations in ılk and on a surface. Then, using the Hamilton (the least action) variational principle we the complete set of governing equations.

quations in the bulk

consider an elastic solid which occupies in a reference placement volume V with the lary $A = \partial V$. A deformation of the solid is described as a mapping from reference placement ie current one

$$\mathbf{x} = \mathbf{x}(\mathbf{X}, t), \tag{2.1}$$

where $\mathbf{x}$ and $\mathbf{X}$ are the position vectors in the current and reference placements, respectively, and t is time. In what follows we use the direct (coordinate-free) tensor calculus as presented in [46, 47]. For hyperelastic solids, there exists a strain energy density W as a function of deformation gradient $\mathbf{F}$

$$W = W(\mathbf{F}) \quad \text{and} \quad \mathbf{F} = \nabla \mathbf{x}, \tag{2.2}$$

where ∇ is the three-dimensional nabla-operator. For example, with Cartesian coordinates X_k, $k = 1, 2, 3$, and corresponding unit orthogonal base vectors $\mathbf{i}_k$, we have

$$\nabla = \mathbf{i}_k \otimes \partial_k, \quad \mathbf{F} = \mathbf{i}_k \otimes \partial_k \mathbf{x} \quad \text{and} \quad \partial_k = \frac{\partial}{\partial X_k},$$

where $\otimes$ denotes the dyadic product and Einstein's summation rule is used. Using the principle of material frame indifference [48], we came to the following form of W:

$$W = W(\mathbf{C}),$$

where $\mathbf{C} = \mathbf{F} \cdot \mathbf{F}^T$ is the Cauchy–Green strain tensor and the dot stands for the scalar product.

In addition to W, we introduce the kinetic energy density as follows:

$$K = \frac{1}{2} \rho \dot{\mathbf{u}} \cdot \dot{\mathbf{u}},$$

where ρ is a referential mass density, $\mathbf{u} = \mathbf{x} - \mathbf{X}$ is the displacement vector, and the overdot denotes the derivative with respect to t. Without mass forces, the Lagrangian equation of motion is given by

$$\nabla \cdot \mathbf{P} = \rho \ddot{\mathbf{u}}, \tag{2.3}$$

where $\mathbf{P} = (\partial W / \partial \mathbf{F}) = 2(\partial W / \partial \mathbf{C}) \cdot \mathbf{F}$ is the first Piola–Kirchhoff stress tensor.

(b) Finite deformations of an elastic beam

Neglecting twisting and transverse shear deformations, we restrict ourselves by a simplest model of a beam undergoing finite motions. We model the beam as an elastic curve with the line strain energy density U_b which depends on the stretch λ and the change of curvature $\varkappa$:

$$U_b = U_b(\lambda, \varkappa). \tag{2.4}$$

The latter are defined as follows. Let $\mathbf{R} = \mathbf{R}(s)$ and $\mathbf{r} = \mathbf{r}(s)$ be position vectors of the curve in reference and current placements, respectively, where s is the referential arc-length of the curve. Then we have the formulae

$$\lambda(s) = |\mathbf{r}'(s)| \quad \text{and} \quad \varkappa(s) = \frac{|\mathbf{r}'(s) \times \mathbf{r}''(s)|}{\lambda^3(s)} - |\mathbf{R}''(s)|, \tag{2.5}$$

where the prime denotes the derivative with respect to s, $\times$ stands for the cross product and the formulae for the curvature of a curve were applied, e.g. [47, p. 115].

an example of the strain energy function, one can consider the following dependence

$$U_b = \frac{1}{2} \mathbb{K}_s (\lambda - 1)^2 + \frac{1}{2} \mathbb{K}_b \varkappa^2, \tag{2.6}$$

$\mathbb{K}_s$ and $\mathbb{K}_b$ are elastic moduli related to tensional and bending stiffness, respectively. ion (2.6) corresponds to a geometrically nonlinear model of a thin beam of symmetric section such as a circular one.

urface strain energy density

the point of view of structural mechanics, the Gurtin–Murdoch surface elasticity [8] bes an elastic membrane perfectly attached to a solid boundary or its part. So the surface es can be interpreted as a membrane force (stress resultants) in the membrane. Here we ler an elastic membrane reinforced by elastic beams aligned along a preferred direction. In order to introduce the model, let us recall some preliminary notations from differential geometry [46,47]. Treating a deformation of the membrane as a mapping from reference placement into a current one, we consider two surfaces Ω and ω with the corresponding position vectors $\mathbf{R}$ and $\mathbf{r}$. So the vectorial parameterizations of Ω and ω are given by

$$\mathbf{R} = \mathbf{R}(s_1, s_2) \quad \text{and} \quad \mathbf{r} = \mathbf{r}(s_1, s_2).$$

Here s_1 and s_2 are surface coordinates on Ω, which are also used for the parametrization of ω. We introduce the surface nabla-operator ∇_s by the relations

$$\nabla_s = \mathbf{R}^\alpha \otimes \partial_\alpha, \quad \mathbf{R}^\alpha \cdot \mathbf{R}_\beta = \delta^\alpha_\beta, \quad \mathbf{R}_\beta = \partial_\beta \mathbf{R}, \quad \mathbf{N} = \frac{\mathbf{R}_1 \times \mathbf{R}_2}{|\mathbf{R}_1 \times \mathbf{R}_2|}, \quad \mathbf{R}^\alpha \cdot \mathbf{N} = 0, \quad \partial_\alpha = \frac{\partial}{\partial s_\alpha},$$

where δ^α_β is the Kronecker symbol, $\alpha, \beta = 1, 2$, and $\mathbf{N}$ is the unit vector of normal to Ω. There is a simple relation between ∇_s and ∇ given by the formula $\nabla_s = \mathbf{A} \cdot \nabla$, where $\mathbf{A} = \mathbf{I} - \mathbf{N} \otimes \mathbf{N}$ is the metric tensor and $\mathbf{I}$ is the three-dimensional unit tensor. So the surface deformation gradient is defined as $\mathbf{F}_s = \nabla_s \mathbf{r}$.

Let us consider a family of N aligned thin long elastic beams attached to a part of the boundary $S \subset A = \partial V$. We introduce surface coordinates s_1 and s_2 such that $s_1 = s$ is the referential arc-length parameter along the beam axis, while s_2 is chosen to be orthogonal to s_1-curves. For s_1 and s_2, we also introduce correspondent unit tangent vectors $\boldsymbol{\tau}$ and $\boldsymbol{\nu}$. Note that $\boldsymbol{\tau} = \partial_1 \mathbf{R}$. So we have the following vectorial parameterizations of the family

$$\mathbf{R} = \mathbf{R}(s_1, s_2), \quad \mathbf{r} = \mathbf{r}(s_1, s_2), \; s_2 = s_2^{(i)}, \; i = 1 \ldots N,$$

related to the reference and current placements, respectively. Note that here s_2 takes a finite set of values and plays a role of a parameter which distinguishes beams in the family.

Instead of studying the discrete system of beams in the following, we consider an averaged coating. In other words, we replace a finite set of beams by infinite one, so at any point (s_1, s_2), there is a beam directed along s_1-curve. With this description λ and $\varkappa$ introduced above through (2.5) take the form

$$\begin{aligned}\lambda = \lambda(s_1, s_2) = |\partial_1 \mathbf{r}(s_1, s_2)| = |\tau \cdot \nabla_s \mathbf{r}(s_1, s_2)| = |\boldsymbol{\tau} \cdot \mathbf{F}_s| \\ = (\boldsymbol{\tau} \cdot \mathbf{C}_s \cdot \boldsymbol{\tau})^{1/2},\end{aligned} \tag{2.7}$$

and

$$\begin{aligned}\varkappa = \varkappa(s_1, s_2) &= \frac{|\partial_1 \mathbf{r}(s_1, s_2) \times \partial_1^2 \mathbf{r}(s_1, s_2)|}{\lambda^3(s_1, s_2)} - |\partial_1 \boldsymbol{\tau}(s_1, s_2)| \\ &= \frac{\left|(\boldsymbol{\tau} \cdot \mathbf{F}_s) \times \left(\varkappa_0 \boldsymbol{\nu} \cdot \mathbf{F}_s + \boldsymbol{\tau} \cdot (\boldsymbol{\tau} \cdot \nabla_s \mathbf{F}_s)\right)\right|}{(\boldsymbol{\tau} \cdot \mathbf{C}_s \cdot \boldsymbol{\tau})^{3/2}} - \varkappa_0,\end{aligned} \tag{2.8}$$

: $\mathbf{C}_s = \mathbf{F}_s \cdot \mathbf{F}_s^T$ is the surface Cauchy–Green strain tensor, the Frenet–Serret formulae are used,

$$\boldsymbol{\tau} = \partial_1 \mathbf{R} \quad \text{and} \quad \partial_1 \boldsymbol{\tau} = \varkappa_0 \boldsymbol{\nu}$$

$_0 \equiv |\partial_1 \boldsymbol{\tau}|$ is the referential curvature of a beam. So the stretching/elongation along beams e described with $\mathbf{C}_s$. Let us recall that for a nonlinear elastic membrane, a surface strain y density is a function of $\mathbf{C}_s$ only, e.g. [8]. Unlike λ, $\varkappa$ cannot be expressed through $\mathbf{C}_s$ and rvature tensors of Ω and ω, in general. It can be expressed through $\mathbf{F}_s$ and its first gradients. general constitutive dependence can be called the surface strain-gradient elasticity with

$$W_s = W_s(\mathbf{F}_s, \nabla_s \mathbf{F}_s). \tag{2.9}$$

cording to (2.8), here the third-order tensor $\nabla_s \mathbf{F}_s$ is present through a scalar only. This onal parameter $\varkappa$ can be treated as a surface bending strain measure. As a result, the surface strain energy is assumed as

$$W_s = W_s(\mathbf{C}_s, \varkappa; \boldsymbol{\tau} \otimes \boldsymbol{\tau}), \tag{2.10}$$

where $\boldsymbol{\tau} \otimes \boldsymbol{\tau}$ plays a role of a structural tensor as in the case of fibre-reinforced composites [49,50]. With the theory of invariants, W_s can be represented as a function of joint invariants

$$W_s = W_s(\mathrm{tr}\mathbf{C}_s, \mathrm{tr}\mathbf{C}_s^2, \boldsymbol{\tau} \cdot \mathbf{C}_s \cdot \boldsymbol{\tau}, \varkappa), \tag{2.11}$$

where tr is the trace operator, see [49–51] for more detail. As an example, the following quadratic function can be used as a geometrically nonlinear two-dimensional medium

$$W_s = \mathbb{K}_1 \mathrm{tr}(\mathbf{E}^2) + \frac{1}{2}\mathbb{K}_2(\mathrm{tr}\mathbf{E})^2 + \frac{1}{2}\mathbb{K}_3(\boldsymbol{\tau} \cdot \mathbf{E} \cdot \boldsymbol{\tau})^2 + \frac{1}{2}\mathbb{K}_4(\boldsymbol{\tau} \cdot \mathbf{E} \cdot \boldsymbol{\tau})(\mathrm{tr}\mathbf{E}) + \frac{1}{2}\mathbb{K}_b \varkappa^2, \tag{2.12}$$

$$\mathbf{E} = \frac{1}{2}(\mathbf{C}_s - \mathbf{A}),$$

where $\mathbb{K}_1$, $\mathbb{K}_2$, $\mathbb{K}_3$, $\mathbb{K}_4$ and $\mathbb{K}_b$ are surface elastic moduli. Equation (2.12) can be called the Saint Venant–Kirchhoff anisotropic membrane model.

For simplicity, we neglect here the rotatory inertia of the beams, so the surface kinetic energy density becomes defined as in [9]

$$K_s = \frac{1}{2} m \dot{\mathbf{u}} \cdot \dot{\mathbf{u}}, \tag{2.13}$$

where m is the referential surface mass density. Let us note (2.13) one of the main assumptions as it results in the appearance of the surface anti-plane waves. Including the rotatory inertia may lead to gradient terms in the kinetic energy as in the Toupin–Mindlin strain-gradient elasticity and may change the dispersion relations, e.g. [36].

Finally, to complete a model, we assume the kinematic compatibility condition relating position vectors $\mathbf{r}$ of the surface and $\mathbf{x}$ in the bulk

$$\mathbf{r} = \mathbf{x}\big|_S. \tag{2.14}$$

Some possible extensions of (2.14) for microstructural coatings were discussed in [14].

(d) Generalized Laplace–Young equation

In order to derive natural boundary conditions, we apply the least action principle [52] modified for surface elasticity as in [53]. The least action functional takes the form

$$\mathcal{H}[\mathbf{x}] = \int_{t_1}^{t_2} \iiint_V (K - W)\,\mathrm{d}V\,\mathrm{d}t + \int_{t_1}^{t_2} \iint_S (K_s - W_s)\,\mathrm{d}A\,\mathrm{d}t, \tag{2.15}$$

where t_1 and t_2 are two time instants, where the variations of $\mathbf{x}$ are assumed to be zero: $\delta\mathbf{x}|_{t=t_1} =$ $= \mathbf{0}$. Considering the variational equation

$$\delta\mathcal{H} = 0, \tag{2.16}$$

n derive the motion equation in the bulk and the natural boundary condition on S. Using ındard technique of calculus of variations from (2.16), we get the motion equation (2.3) and namic boundary conditions on S and along $\ell = \partial S$. Indeed, after integration by part, we get

$$\delta \int_{t_1}^{t_2} \iiint_V (K - W)\,\mathrm{d}V\,\mathrm{d}t = \int_{t_1}^{t_2} \iiint_V (-\rho\ddot{\mathbf{u}} + \nabla \cdot \mathbf{P}) \cdot \delta\mathbf{x}\,\mathrm{d}V\,\mathrm{d}t - \int_{t_1}^{t_2} \iint_A \mathbf{N} \cdot \mathbf{P} \cdot \delta\mathbf{x}\,\mathrm{d}A\,\mathrm{d}t. \tag{2.17}$$

dering $\delta\mathbf{x} = \mathbf{0}$ on A from (2.16) and (2.17) we have that

$$\int_{t_1}^{t_2} \iiint_V (-\rho\ddot{\mathbf{u}} + \nabla \cdot \mathbf{P}) \cdot \delta\mathbf{x}\,\mathrm{d}V\,\mathrm{d}t = 0$$

which is a weak form of (2.3). For the beginning we consider W_s in form (2.9). Now $\delta\mathcal{H}$ take the form

$$\delta\mathcal{H} = -\int_{t_1}^{t_2}\iint_A \mathbf{N}\cdot\mathbf{P}\cdot\delta\mathbf{x}\,\mathrm{d}A\,\mathrm{d}t - \int_{t_1}^{t_2}\iint_S m\ddot{\mathbf{u}}\cdot\delta\mathbf{x}\,\mathrm{d}A\,\mathrm{d}t$$
$$-\int_{t_1}^{t_2}\iint_S \left(\frac{\partial W_s}{\partial\mathbf{F}_s} : \delta\mathbf{F}_s + \frac{\partial W_s}{\partial\nabla_s\mathbf{F}_s} \therefore \delta\nabla_s\mathbf{F}_s\right)\mathrm{d}A\,\mathrm{d}t,$$

where the double-dot and the triple-dot products stand for inner (scalar) in the space of second- and third-order tensors, respectively. We introduce surface first Piola–Kirchhoff-type stress $\mathbf{S}$ and hyperstress $\mathbf{M}$ tensors by the formulae

$$\mathbf{S} = \frac{\partial W_s}{\partial\mathbf{F}_s} = 2\frac{\partial W_s}{\partial\mathbf{C}_s}\cdot\mathbf{F}_s \quad\text{and}\quad \mathbf{M} = \frac{\partial W_s}{\partial\nabla_s\mathbf{F}_s}.$$

As $\varkappa$ depends on both $\mathbf{F}_s$ and $\nabla_s\mathbf{F}_s$ here both tensors $\mathbf{S}$ and $\mathbf{M}$ depend also on $\mathbf{F}_s$ and $\nabla_s\mathbf{F}_s$. In other words, there is a coupling between strains and strain gradient, and between stresses and hyperstresses. Note that they have the following properties: $\mathbf{N}\cdot\mathbf{S}=\mathbf{0}$, $\mathbf{N}\cdot\mathbf{M}=\mathbf{0}$ and $\mathbf{N}\cdot(\mathbf{a}\cdot\mathbf{M}) = \mathbf{0}$, for any vector $\mathbf{a}$, which are important for integration by part. For example, $\mathbf{M}$ takes rather awkward form

$$\mathbf{M} = \frac{\boldsymbol{\tau}\otimes\boldsymbol{\tau}\otimes\left[\boldsymbol{\tau}\cdot\mathbf{F}_s\times(\boldsymbol{\tau}\otimes\boldsymbol{\tau}:\nabla_s\mathbf{F}_s)\times\mathbf{F}_s^T\cdot\boldsymbol{\tau}\right]}{\left|(\boldsymbol{\tau}\cdot\mathbf{F}_s)\times\left(\varkappa_0\boldsymbol{\nu}\cdot\mathbf{F}_s+\boldsymbol{\tau}\cdot(\boldsymbol{\tau}\cdot\nabla_s\mathbf{F}_s)\right)\right|(\boldsymbol{\tau}\cdot\mathbf{C}_s\cdot\boldsymbol{\tau})^{3/2}}\frac{\partial W_s}{\partial\varkappa},$$

which also demonstrates a strong anisotropy of surface properties.

In what follows we assume that the contour $\ell = \partial S$ is closed and smooth enough that is without corners. In order to perform the further integration by part, we use the surface divergence theorem [8,47], which states that

$$\iint_S (\nabla_s\cdot\mathbf{X} + 2H\mathbf{N}\cdot\mathbf{X})\,\mathrm{d}A = \int_\ell \mathbf{m}\cdot\mathbf{X}\,\mathrm{d}s, \tag{2.18}$$

where $\mathbf{X}$ is a continuously differentiable tensor-valued field given on S with the smooth contour $\ell = \partial S$, $\mathbf{m}$ is the unit normal to ℓ such that $\mathbf{m}\cdot\boldsymbol{\tau} = \mathbf{m}\cdot\mathbf{N} = 0$, and $H = -\frac{1}{2}\nabla_s\cdot\mathbf{N}$ is the mean curvature of S. Using (2.18), we get the following formula of integration by parts

$$\iint_S \mathbf{X}:\nabla_s\mathbf{y}\,\mathrm{d}A = \int_\ell \mathbf{m}\cdot\mathbf{X}\cdot\mathbf{y}\,\mathrm{d}s - \int_S\left[(\nabla_s\cdot\mathbf{X})\cdot\mathbf{y} + 2H\mathbf{N}\cdot\mathbf{X}\cdot\mathbf{y}\right]\mathrm{d}A \tag{2.19}$$

for any fields $\mathbf{X}$ and $\mathbf{y}$ defined on S. With (2.19), we have the identities

$$\begin{aligned}
\delta\iint_S W_s\,\mathrm{d}A &= \iint_S (\mathbf{S}:\delta\mathbf{F}_s + \mathbf{M}\therefore\delta\nabla_s\mathbf{F}_s)\,\mathrm{d}A\\
&= \iint_S [-(\nabla_s\cdot\mathbf{S})\cdot\delta\mathbf{x} - (\nabla_s\cdot\mathbf{M}):\nabla_s\delta\mathbf{x}]\,\mathrm{d}A + \int_\ell (\mathbf{m}\cdot\mathbf{S}\cdot\delta\mathbf{x} + \mathbf{m}\cdot\mathbf{M}:\nabla_s\delta\mathbf{x})\,\mathrm{d}s\\
&= \iint_S [-\nabla_s\cdot\mathbf{S} + \nabla_s\cdot(\nabla_s\cdot\mathbf{M}) + 2H\mathbf{N}\cdot(\nabla_s\cdot\mathbf{M})]\cdot\delta\mathbf{x}\,\mathrm{d}A\\
&\quad + \int_\ell (\mathbf{m}\cdot\mathbf{S}\cdot\delta\mathbf{x} + \mathbf{m}\cdot\mathbf{M}:\nabla_s\delta\mathbf{x} - \mathbf{m}\cdot(\nabla_s\cdot\mathbf{M})\cdot\delta\mathbf{x})\,\mathrm{d}s\\
&= \iint_S [-\nabla_s\cdot\mathbf{S} + \nabla_s\cdot(\nabla_s\cdot\mathbf{M}) + 2H\mathbf{N}\cdot(\nabla_s\cdot\mathbf{M})]\cdot\delta\mathbf{x}\,\mathrm{d}A\\
&\quad + \int_\ell (\mathbf{m}\cdot\mathbf{S}\cdot\delta\mathbf{x} + \mathbf{m}\cdot\mathbf{M}:\nabla_s\delta\mathbf{x} - \mathbf{m}\cdot(\nabla_s\cdot\mathbf{M})\cdot\delta\mathbf{x})\,\mathrm{d}s.
\end{aligned}$$

esult, from (2.16), we have the natural boundary condition on A

$$\mathbf{N}\cdot\mathbf{P} = \mathbf{0}, \quad \mathbf{x}\in A\setminus S \tag{2.20}$$

$$\mathbf{N}\cdot\mathbf{P} = \nabla_s\cdot\mathbf{S} - \nabla_s\cdot(\nabla_s\cdot\mathbf{M}) - 2H\mathbf{N}\cdot(\nabla_s\cdot\mathbf{M}) - m\ddot{\mathbf{x}}, \quad \mathbf{x}\in S, \tag{2.21}$$

and along ℓ

$$\mathbf{m} \cdot (\mathbf{m} \cdot \mathbf{M}) = \mathbf{0} \quad \text{and} \quad \mathbf{m} \cdot \mathbf{S} = \mathbf{m} \cdot (\nabla_s \cdot \mathbf{M}) + \frac{\partial}{\partial s}(\mathbf{m} \cdot \mathbf{M} \cdot \boldsymbol{\tau}). \tag{2.22}$$

Here (2.21) plays a role of the Laplace–Young equation in the theory of capillarity, so it can be called the generalized Laplace–Young equation. For statics, equations (2.21) and (2.22) have the form similar to the boundary conditions within the linear Steigmann–Ogden model [15] but with different constitutive equations for the surface stress measures. For $\mathbf{M} = \mathbf{0}$, equation (2.21) coincides with the boundary condition within the Gurtin–Murdoch model [8].

3. Small deformations for a flat boundary with straight beams

For some applications such as an acoustic wave propagation, we can restrict ourselves by infinitesimal deformations. In this case, we have

$$\mathbf{C} \approx \mathbf{I} + 2\mathbf{e}, \quad \mathbf{e} = \frac{1}{2}\left(\nabla\mathbf{u} + (\nabla\mathbf{u})^T\right),$$

$$\mathbf{C}_s \approx \mathbf{A} + 2\boldsymbol{\epsilon}, \quad \mathbf{E} = \boldsymbol{\epsilon}, \quad \boldsymbol{\epsilon} = \frac{1}{2}\left(\nabla_s\mathbf{u} \cdot \mathbf{A} + \mathbf{A} \cdot (\nabla_s\mathbf{u})^T\right), \quad \lambda \approx 1 + \boldsymbol{\tau} \cdot \boldsymbol{\epsilon} \cdot \boldsymbol{\tau} = 1 + \boldsymbol{\tau} \cdot \nabla_s\mathbf{u} \cdot \boldsymbol{\tau}.$$

For an isotropic in the bulk solid, we get the Hooke Law

$$W = \frac{1}{2}\tilde{\lambda}(\operatorname{tr}\mathbf{e})^2 + \mu \operatorname{tr}(\mathbf{e} \cdot \mathbf{e}) \quad \text{and} \quad \mathbf{P} = \tilde{\lambda}\mathbf{I} \operatorname{tr}\mathbf{e} + 2\mu\mathbf{e}, \tag{3.1}$$

where $\tilde{\lambda}$ and μ are the Lamé moduli.

For simplicity, let us consider flat surface S and straight beams. So we have $\varkappa_0 = 0$, $\boldsymbol{\tau} = \mathbf{i}_1 =$ const, and

$$\varkappa = |\boldsymbol{\tau} \times (\boldsymbol{\tau} \cdot \nabla_s)(\boldsymbol{\tau} \cdot \nabla_s)\mathbf{u}|. \tag{3.2}$$

With these approximations, the surface strain energy density became similar to (2.12)

$$W_s = \mathbb{K}_1 \operatorname{tr}(\boldsymbol{\epsilon}^2) + \frac{1}{2}\mathbb{K}_2(\operatorname{tr}\boldsymbol{\epsilon})^2 + \frac{1}{2}\mathbb{K}_3(\boldsymbol{\tau} \cdot \boldsymbol{\epsilon} \cdot \boldsymbol{\tau})^2 + \frac{1}{2}\mathbb{K}_4(\boldsymbol{\tau} \cdot \boldsymbol{\epsilon} \cdot \boldsymbol{\tau})(\operatorname{tr}\boldsymbol{\epsilon})$$
$$+ \frac{1}{2}\mathbb{K}_b\left[\boldsymbol{\tau} \times (\boldsymbol{\tau} \cdot \nabla_s)(\boldsymbol{\tau} \cdot \nabla_s)\mathbf{u}\right] \cdot \left[\boldsymbol{\tau} \times (\boldsymbol{\tau} \cdot \nabla_s)(\boldsymbol{\tau} \cdot \nabla_s)\mathbf{u}\right], \tag{3.3}$$

whereas the surface stress and hyperstress tensors take the form

$$\mathbf{S} = \frac{\partial W_s}{\partial \boldsymbol{\epsilon}} = 2\mathbb{K}_1\boldsymbol{\epsilon} + (\mathbb{K}_2 \operatorname{tr}\boldsymbol{\epsilon} + \mathbb{K}_4\boldsymbol{\tau} \cdot \boldsymbol{\epsilon} \cdot \boldsymbol{\tau})\,\mathbf{A} + (\mathbb{K}_3\boldsymbol{\tau} \cdot \boldsymbol{\epsilon} \cdot \boldsymbol{\tau} + \mathbb{K}_4 \operatorname{tr}\boldsymbol{\epsilon})\,\boldsymbol{\tau} \otimes \boldsymbol{\tau} \tag{3.4}$$

and

$$\mathbf{M} = \frac{\partial W_s}{\partial \nabla_s\nabla_s\mathbf{u}} = \mathbb{K}_b\boldsymbol{\tau} \otimes \boldsymbol{\tau} \otimes \{\boldsymbol{\tau} \times [(\boldsymbol{\tau} \otimes \boldsymbol{\tau}) : \nabla_s\nabla_s\mathbf{u}]\} \times \boldsymbol{\tau}. \tag{3.5}$$

Unlike the nonlinear case, here $\mathbf{S}$ depends on the first gradient of displacements only, whereas $\mathbf{M}$ i a linear function of the second gradient. Obviously, for any vector $\mathbf{m}$ orthogonal to $\boldsymbol{\tau}$, we have $\cdot \mathbf{M} = \mathbf{0}$. So for an edge with the normal $\mathbf{m}$ that is an edge parallel to the beams, the edge tion (2.22)$_1$ is fulfilled, whereas (2.22)$_2$ transforms into $\mathbf{m} \cdot \mathbf{S} = \mathbf{0}$.

nti-plane surface waves

usly, the presented model relates to strong anisotropy in surface properties. In order to nstrate its influence, let us analyse a surface anti-plane wave propagation. Recently, the sis of cloaking with respect to anti-plane waves was studied in [54] for non-homogeneous essed solids. Within the linear isotropic Gurtin–Murdoch surface elasticity, such analysis erformed in [53]. Following this technique let us consider anti-plane motions in an elastic pace taking into account surface strain energy. Let us introduce the Cartesian coordinates ch that the half-space occupies the region $X_3 \le 0$, equation $X_3 = 0$ describes its boundary, as X_1 corresponds to fibres' direction, see figure 1.

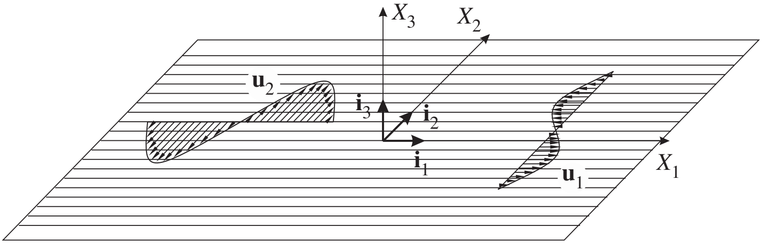

Figure 1. An elastic half-space with surface beam-lattice enhancement.

The anti-plane motions are assumed to be one of the following forms [55]

$$\mathbf{u}_1 = u_1(X_2, X_3, t)\mathbf{i}_1, \quad \text{and} \quad \mathbf{u}_2 = u_2(X_1, X_3, t)\mathbf{i}_2, \tag{4.1}$$

which corresponds to two different directions of a wave propagation. For (4.1), we have the formulae

$$\left.\begin{aligned}
&\nabla\mathbf{u}_1 = (\partial_2 u_1\mathbf{i}_2 + \partial_3 u_1\mathbf{i}_3)\otimes\mathbf{i}_1, \quad \nabla_s\mathbf{u}_1 = \partial_2 u_1\mathbf{i}_2\otimes\mathbf{i}_1, \quad \nabla_s\nabla_s\mathbf{u}_1 = \partial_2^2 u_1\mathbf{i}_2\otimes\mathbf{i}_2\otimes\mathbf{i}_1,\\
&\nabla\mathbf{u}_2 = (\partial_1 u_2\mathbf{i}_1 + \partial_3 u_2\mathbf{i}_3)\otimes\mathbf{i}_2, \quad \nabla_s\mathbf{u}_2 = \partial_1 u_2\mathbf{i}_1\otimes\mathbf{i}_2, \quad \nabla_s\nabla_s\mathbf{u}_2 = \partial_1^2 u_2\mathbf{i}_1\otimes\mathbf{i}_1\otimes\mathbf{i}_2,\\
&\mathbf{P}(\mathbf{u}_1) = \mu\left[\partial_2 u_1(\mathbf{i}_1\otimes\mathbf{i}_2 + \mathbf{i}_2\otimes\mathbf{i}_1) + \partial_3 u_1(\mathbf{i}_1\otimes\mathbf{i}_3 + \mathbf{i}_3\otimes\mathbf{i}_1)\right],\\
&\mathbf{P}(\mathbf{u}_2) = \mu\left[\partial_1 u_2(\mathbf{i}_1\otimes\mathbf{i}_2 + \mathbf{i}_2\otimes\mathbf{i}_1) + \partial_3 u_2(\mathbf{i}_2\otimes\mathbf{i}_3 + \mathbf{i}_3\otimes\mathbf{i}_2)\right],\\
&\mathbf{S}(\mathbf{u}_1) = \mathbb{K}_1\partial_2 u_1(\mathbf{i}_1\otimes\mathbf{i}_2 + \mathbf{i}_2\otimes\mathbf{i}_1), \quad \mathbf{S}(\mathbf{u}_2) = \mathbb{K}_1\partial_1 u_2(\mathbf{i}_1\otimes\mathbf{i}_2 + \mathbf{i}_2\otimes\mathbf{i}_1)\\
\text{and}\quad &\mathbf{M}(\mathbf{u}_1) = \mathbf{0}, \quad \mathbf{M}(\mathbf{u}_2) = \mathbb{K}_b\partial_1^2 u_2\mathbf{i}_1\otimes\mathbf{i}_1\otimes\mathbf{i}_2.
\end{aligned}\right\} \tag{4.2}$$

As $\mathbf{M}(\mathbf{u}_1) = \mathbf{0}$ while $\mathbf{M}(\mathbf{u}_2) \neq \mathbf{0}$, $\mathbf{u}_1$ describes shear motions without beam bending, whereas $\mathbf{u}_2$ includes bending deformations of the beams, see figure 1.

With (4.1) and (4.2), the general equations of motion reduce into two wave equations with respect to u_1 and u_2, respectively,

$$\mu(\partial_2^2 + \partial_3^2)u_1 = \rho\ddot{u}_1 \tag{4.3}$$

and

$$\mu(\partial_1^2 + \partial_3^2)u_2 = \rho\ddot{u}_2. \tag{4.4}$$

Corresponding to (4.3) and (4.4) natural boundary conditions have the form

$$\mu\partial_3 u_1 = -m\ddot{u}_1 + \mathbb{K}_1\partial_2^2 u_1 \tag{4.5}$$

and

$$\mu\partial_3 u_2 = -m\ddot{u}_2 + \mathbb{K}_1\partial_1^2 u_2 - \mathbb{K}_b\partial_1^4 u_2, \tag{4.6}$$

...ctively. Equation (4.5) corresponds to the boundary condition within the Gurtin–Murdoch ...l in the case of anti-plane deformations [53], whereas equation (4.6) includes additional ...describing the bending energy as in [56]. So we call this anti-plane motion the bending ...nt mode. Note that we have different boundary conditions depending on the reinforcement ...ion.

...suming a steady state and looking for the solution of (4.3) and (4.4) in the form

$$u_1 = U_1(X_2, X_3)\exp(i\omega t) \quad \text{and} \quad u_2 = U_2(X_1, X_3)\exp(i\omega t), \tag{4.7}$$

... ω is a circular frequency, i is the imaginary unit and U_α is an amplitude, $\alpha = 1, 2$. With (4.7) ...ions (4.3) and (4.4) transform into

$$\mu(\partial_2^2 + \partial_3^2)U_1 = -\rho\omega^2 U_1 \quad \text{and} \quad \mu(\partial_1^2 + \partial_3^2)U_2 = -\rho\omega^2 U_2. \tag{4.8}$$

Decaying at $X_3 \to -\infty$ solutions of (4.8) are given by

$$U_1 = U_{01}\exp(\varkappa X_3)\exp(ikX_2) \quad \text{and} \quad U_2 = U_{02}\exp(\varkappa X_3)\exp(ikX_1), \tag{4.9}$$

where

$$\varkappa = \varkappa(k,\omega) \equiv \sqrt{k^2 - \frac{\omega^2}{c_T^2}} \quad \text{and} \quad c_T = \sqrt{\frac{\mu}{\rho}},$$

k is a wavenumber, c_T is the phase velocity of transverse waves in the bulk, and $U_{0\alpha}$ are constants. Substituting (4.7) with (4.9) into (4.5) and (4.6), we get the dispersion relations

$$\mu\varkappa(k,\omega) = m\omega^2 - \mathbb{K}_1 k^2 \tag{4.10}$$

and

$$\mu\varkappa(k,\omega) = m\omega^2 - \mathbb{K}_1 k^2 + \mathbb{K}_b k^4. \tag{4.11}$$

These equations can be transformed into

$$c^2 = c_s^2 + \frac{\mu}{m}\frac{1}{|k|}\sqrt{1 - \frac{c^2}{c_T^2}} \tag{4.12}$$

and

$$c^2 = c_s^2 + \frac{\mathbb{K}_b}{m}k^2 + \frac{\mu}{m}\frac{1}{|k|}\sqrt{1 - \frac{c^2}{c_T^2}}, \tag{4.13}$$

where $c_s = \sqrt{\mathbb{K}_1/m}$ is the surface shear wave velocity within the Gurtin–Murdoch model [53] and $c = \omega/k$ the phase velocity. Dispersion relations (4.12) and (4.11) were analysed in [53,56], respectively. Here (4.10) or (4.12) describes the dispersion of the surface anti-plane wave propagating along surface fibres whereas (4.11) or (4.13) relates to the surface anti-plane wave propagating across surface fibres. The dispersion curve for (4.12) is shown in figure 2, see the dashed red curve GM. Here $\bar{k}$ and $\bar{\mathbb{K}}$ are normalized (dimensionless) wavenumber and the bending stiffness, respectively, introduced by the formulae

$$\bar{k} = \frac{c_T^2 m}{\mu}k \quad \text{and} \quad \bar{\mathbb{K}} = \frac{\mu^2}{m^3 c_T^6}\mathbb{K}_b.$$

Note that the ratio $p = \rho/m \equiv c_T^2 m/\mu$ constitutes the characteristic wavenumber within the Gurtin–Murdoch model, so $\bar{k} = k/p$. This surface wave exists in the range

$$c_s < c(k) \le c_T \quad \forall\ k.$$

We have the relations $c(0) = c_T$ and $c \to c_s$ as $k \to \infty$. So for long waves ($k \approx 0$) there is no influence of surface elasticity, it becomes definitive at short waves as it should be.

The term $\mathbb{K}_b k^2$, which is responsible for bending stiffness of beams, changes dramatically the behaviour of dispersion curves related to (4.13), see figure 2, where curves 1–4 correspond to the following values of $\bar{\mathbb{K}}$: $\bar{\mathbb{K}} = 10^{-1}$; 10^{-2}; 10^{-3}; 10^{-4}, respectively. For relatively small values of k, ...spersion curves almost coincide with the GM curve, then c grows until c_T. In other words, ...a fixed range $0 \le k \le k_1$, the dispersion curves of the bending resistant mode for $\bar{\mathbb{K}} \to 0$ ...ome arbitrarily close to the dispersion curve of the Gurtin–Murdoch model. For $\bar{\mathbb{K}}$ fixed the ...s approach the line $c = c_T$ at $k = k_{\max}$, where $k_{\max}$ takes the value

$$k_{\max} = \sqrt{\frac{c_T^2 - c_s^2}{\mathbb{K}_b}},$$

...the Gurtin–Murdoch dispersion curve tends to the velocity c_s as $k \to \infty$. At $k = k_{\max}$, phase ...ty is equal c_T, see the vertical dashed line for $\bar{\mathbb{K}} = 10^{-3}$ in figure 2. So for the bending ...nt mode, the anti-plane surface wave exists if $0 \le k \le k_{\max}$. Thus, the bending stiffness ...es the condition of the existence of anti-plane surface waves. For long waves (small k), ...is no influence of bending stiffness, whereas for short waves, we get completely different ...iour than observed for the Gurtin–Murdoch model.

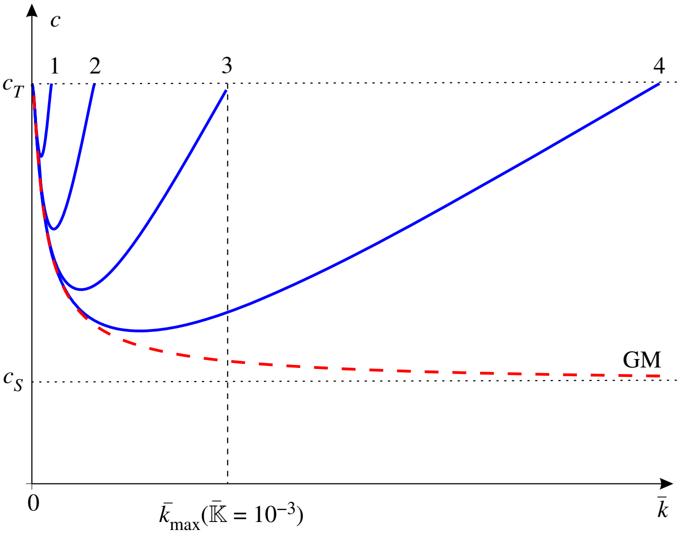

Figure 2. Dispersion curves. The red dashed curve corresponds to the Gurtin–Murdoch model, whereas the numbered blue solid curves relate to the considered bending resistant model. Here *N*th curve corresponds to $\mathbb{K} = 10^{-N}$, $N = 1, 2, 3, 4$. The vertical dashed line relates to the maximal wavenumber $k_{\max}$ for $\mathbb{K} = 10^{-3}$. (Online version in colour.)

5. Conclusion

The new strongly anisotropic model of surface elasticity was introduced, which was motivated by consideration of coatings made of interacting long flexible fibres attached to a boundary. The developed model constitutes a class of surface elasticity which is in between Gurtin–Murdoch and Steigmann–Ogden models [8–11]. Indeed, the introduced surface strain energy is similar to one-dimensional version of the Steigmann–Ogden model [10] but applied to two-dimensional surfaces. From the mechanical point of view, the surface constitutive equations correspond to an elastic membrane reinforced in a preferred direction by elastic beams. Note that here we restricted ourselves to the simplest model of a nonlinear beam. In the forthcoming papers, more complex models based on the directed curve model can be also applied considering rotatory inertia, shear and torsional deformations. Obviously, it results in strongly anisotropic constitutive equations for surface stresses and couples as in the case of fibre-reinforced materials [49,50]. So the model describes finite deformations of an elastic solid with perfectly attached reinforced membrane. Let us note that the model of strongly anisotropic surface elasticity developed here has some similarities with the models of lattice shells made of two families of elastic fibres [57–59].

Using the Hamilton variational principle, we derive the dynamic boundary conditions at ...dary as well as at edges. Considering anti-plane motions within the linearized model, ...alysed a surface anti-plane wave propagation along and across the fibre directions. The ...ponding dispersion relations are derived. In particular, it was shown that the dispersion ...on significantly depends on the direction of the wave propagation. The presented results ...nstrated a significant influence of a surface microstructure on surface waves. Let us note that ...opagating waves in microstructured solids is one of the favourite subjects of Prof. Leonid I. ...an, to whom this paper is devoted, see the seminal works [26,60,61].

...essibility. This article does not contain any additional data.
...ng interests. I declare I have no competing interests.
... The author acknowledges the support of the Government of the Russian Federation (contract no. ....31.0031).
...edgements. The author acknowledges Prof. Gennady Mishuris and all participants of the workshop ...nic Phenomena in Media with Microstructure' held on the occasion of 90th birthday of Prof. Leonid ...n at Tel-Aviv University 7–12 October 2018 for the fruitful and highly motivated discussions.

References

1. Holloway CL, Kuester EF, Gordon JA, O'Hara J, Booth J, Smith DR. 2012 An overview of the theory and applications of metasurfaces: the two-dimensional equivalents of metamaterials. *IEEE Antennas Propag. Mag.* **54**, 10–35. (doi:10.1109/MAP.2012.6230714)
2. Chen HT, Taylor AJ, Yu N. 2016 A review of metasurfaces: physics and applications. *Rep. Prog. Phys.* **79**, 076401. (doi:10.1088/0034-4885/79/7/076401)
3. Maradudin AA (ed.). 2011 *Structured surfaces as optical metamaterials*. Cambridge, UK: Cambridge University Press.
4. Cui TJ, Tang WX, Yang XM, Mei ZL, Jiang WX. 2016 *Metamaterials: beyond crystals, noncrystals, and quasicrystals*. Boca Raton, FL: CRC Press.
5. Bhushan B, Jung YC, Koch K. 2009 Micro-, nano- and hierarchical structures for superhydrophobicity, self-cleaning and low adhesion. *Phil. Trans. R. Soc. A* **367**, 1631–1672. (doi:10.1098/rsta.2009.0014)
6. Kang X, Zi WW, Xu ZG, Zhang HL. 2007 Controlling the micro/nanostructure of self-cleaning polymer coating. *Appl. Surf. Sci.* **253**, 8830–8834. (doi:10.1016/j.apsusc.2007.04.021)
7. Norris AN. 2008 Acoustic cloaking theory. *Proc. R. Soc. A* **464**, 2411–2434. (doi:10.1098/rspa.2008.0076)
8. Gurtin ME, Murdoch AI. 1975 A continuum theory of elastic material surfaces. *Arch. Ration. Mech. Anal.* **57**, 291–323. (doi:10.1007/BF00261375)
9. Gurtin ME, Murdoch AI. 1978 Surface stress in solids. *Int. J. Solids Struct.* **14**, 431–440. (doi:10.1016/0020-7683(78)90008-2)
10. Steigmann DJ, Ogden RW. 1997 Plane deformations of elastic solids with intrinsic boundary elasticity. *Proc. R. Soc. A* **453**, 853–877. (doi:10.1098/rspa.1997.0047)
11. Steigmann DJ, Ogden RW. 1999 Elastic surface-substrate interactions. *Proc. R. Soc. A* **455**, 437–474. (doi:10.1098/rspa.1999.0320)
12. Duan HL, Wang J, Karihaloo BL. 2008 Theory of elasticity at the nanoscale. In *Advances in Applied Mechanic*, vol. 42, pp. 1–68. Elsevier.
13. Wang J, Huang Z, Duan H, Yu S, Feng X, Wang G, Zhang W, Wang T. 2011 Surface stress effect in mechanics of nanostructured materials. *Acta Mech. Solida Sin.* **24**, 52–82. (doi:10.1016/S0894-9166(11)60009-8)
14. Eremeyev VA. 2016 On effective properties of materials at the nano- and microscales considering surface effects. *Acta Mech.* **227**, 29–42. (doi:10.1007/s00707-015-1427-y)
15. Zemlyanova AY, Mogilevskaya SG. 2018 Circular inhomogeneity with Steigmann–Ogden interface: local fields, neutrality, and Maxwell's type approximation formula. *Int. J. Solids Struct.* **135**, 85–98. (doi:10.1016/j.ijsolstr.2017.11.012)
16. Han Z, Mogilevskaya SG, Schillinger D. 2018 Local fields and overall transverse properties of unidirectional composite materials with multiple nanofibers and Steigmann–Ogden interfaces. *Int. J. Solids Struct.* **147**, 166–182. (doi:10.1016/j.ijsolstr.2018.05.019)
17. Gei M. 2008 Elastic waves guided by a material interface. *Eur. J. Mech. A-Solid.* **27**, 328–345. (doi:10.1016/j.euromechsol.2007.10.002)
18. Javili A, McBride A, Steinmann P. 2013 Thermomechanics of solids with lower-dimensional energetics: on the importance of surface, interface, and curve structures at the nanoscale. A ıifying review. *Appl. Mech. Rev.* **65**, 010802. (doi:10.1115/1.4023012)

vili A, Steinmann P. 2013 Geometrically nonlinear higher-gradient elasticity with energetic ›oundaries. *J. Mech. Phys. Solids* **61**, 2381–2401. (doi:10.1016/j.jmps.2013.06.005)

acidi L, Rosi G, Giorgio I, Madeo A. 2014 Reflection and transmission of plane waves surfaces carrying material properties and embedded in second-gradient materials. *Math. ech. Solids* **19**, 555–578. (doi:10.1177/1081286512474016)

:nveniste Y, Miloh T. 2001 Imperfect soft and stiff interfaces in two-dimensional elasticity. *ech. Mater.* **33**, 309–323. (doi:10.1016/S0167-6636(01)00055-2)

urdoch AI. 2005 Some fundamental aspects of surface modelling. *J. Elast.* **80**, 33–52. oi:10.1007/s10659-005-9024-2)

goni D, Gei M, Movchan AB. 2008 Dynamics of a prestressed stiff layer on an elastic ılf space: filtering and band gap characteristics of periodic structural models derived ›om long-wave asymptotics. *J. Mech. Phys. Solids* **56**, 2494–2520. (doi:10.1016/j.jmps.2008. .007)

24. Boutin C, Roussillon P. 2006 Wave propagation in presence of oscillators on the free surface. *Int. J. Eng. Sci.* **44**, 180–204. (doi:10.1016/j.ijengsci.2005.10.002)
25. Mishuris GS, Movchan AB, Slepyan LI. 2007 Waves and fracture in an inhomogeneous lattice structure. *Waves Random Complex Media* **17**, 409–428. (doi:10.1080/17455030701459910)
26. Slepyan LI. 2002 *Models and phenomena in fracture mechanics*. Berlin, Germany: Springer.
27. Brun M, Guenneau S, Movchan AB, Bigoni D. 2010 Dynamics of structural interfaces: filtering and focussing effects for elastic waves. *J. Mech. Phys. Solids* **58**, 1212–1224. (doi:10.1016/j.jmps.2010.06.008)
28. Brun M, Movchan AB, Movchan NV. 2010 Shear polarisation of elastic waves by a structured interface. *Contin. Mech. Thermodyn.* **22**, 663–677. (doi:10.1007/s00161-010-0143-z)
29. Mishuris GS, Movchan AB, Slepyan LI. 2009 Localised knife waves in a structured interface. *J. Mech. Phys. Solids* **57**, 1958–1979. (doi:10.1016/j.jmps.2009.08.004)
30. Schwan L, Boutin C. 2013 Unconventional wave reflection due to 'resonant surface'. *Wave Motion* **50**, 852–868. (doi:10.1016/j.wavemoti.2013.02.010)
31. Nieves M, Mishuris G, Slepyan L. 2017 Transient wave in a transformable periodic flexural structure. *Int. J. Solids Struct.* **112**, 185–208. (doi:10.1016/j.ijsolstr.2016.11.012)
32. Kaplunov J, Prikazchikov DA. 2017 Asymptotic theory for Rayleigh and Rayleigh-type waves. *Adv. Appl. Mech.* **50**, 1–106. (doi:10.1016/bs.aams.2017.01.001)
33. Chebakov R, Kaplunov J, Rogerson G. 2016 Refined boundary conditions on the free surface of an elastic half-space taking into account non-local effects. *Proc. R. Soc. A* **472**, 20150800. (doi:10.1098/rspa.2015.0800)
34. Vardoulakis I, Georgiadis HG. 1997 SH surface waves in a homogeneous gradient-elastic half-space with surface energy. *J. Elast.* **47**, 147–165. (doi:10.1023/A:1007433510623)
35. Gourgiotis PA, Georgiadis HG. 2015 Torsional and SH surface waves in an isotropic and homogenous elastic half-space characterized by the Toupin–Mindlin gradient theory. *Int. J. Solids Struct.* **62**, 217–228. (doi:10.1016/j.ijsolstr.2015.02.032)
36. Eremeyev VA, Rosi G, Naili S. 2018 Comparison of anti-plane surface waves in strain-gradient materials and materials with surface stresses. *Math. Mech. Solids* **24**, 2526–2535. (doi:10.1177/1081286518769960)
37. Eremeyev VA, Sharma BL. 2019 Anti-plane surface waves in media with surface structure: discrete vs. continuum model. *Int. J. Eng. Sci.* **143**, 33–38. (doi:10.1016/j.ijengsci.2019.06.007)
38. Spinelli P, Verschuuren MA, Polman A. 2012 Broadband omnidirectional antireflection coating based on subwavelength surface Mie resonators. *Nat. Commun.* **3**, 692. (doi:10.1038/ncomms1691)
39. Yao Y, Yao J, Narasimhan VK, Ruan Z, Xie C, Fan S, Cui Y. 2012 Broadband light management using low-Q whispering gallery modes in spherical nanoshells. *Nat. Commun.* **3**, 664. (doi:10.1038/ncomms1664)
40. Poddubny A, Iorsh I, Belov P, Kivshar Y. 2013 Hyperbolic metamaterials. *Nat. Photonics* **7**, 948–967. (doi:10.1038/nphoton.2013.243)
41. Ji D, Song H, Zeng X, Hu H, Liu K, Zhang N, Gan Q. 2014 Broadband absorption engineering of hyperbolic metafilm patterns. *Sci. Rep.* **4**, 4498. (doi:10.1038/srep04498)
42. High AA, Devlin RC, Dibos A, Polking M, Wild DS, Perczel J, de Leon NP, Lukin MD, Park H. 2015 Visible-frequency hyperbolic metasurface. *Nature* **522**, 192–196. oi:10.1038/nature14477)

P, Dolado I, Alfaro-Mozaz FJ, Casanova F, Hueso LE, Liu S, Edgar JH, Nikitin AY, Vélez S, illenbrand R. 2018 Infrared hyperbolic metasurface based on nanostructured van der Waals aterials. *Science* **359**, 892–896. (doi:10.1126/science.aaq1704)

anesh VA, Raut HK, Nair AS, Ramakrishna S. 2011 A review on self-cleaning coatings. *Mater. Chem.* **21**, 16 304–16 322. (doi:10.1039/c1jm12523k)

aelachvili JN. 2011 *Intermolecular and surface forces*, 3rd edn. Amsterdam, The Netherlands: ademic Press.

mmonds JG. 1994 *A brief on tensor analysis*, 2nd edn. New York, NY: Springer.

emeyev VA, Cloud MJ, Lebedev LP. 2018 *Applications of tensor analysis in continuum echanics*. Hackensack, NJ: World Scientific.

uesdell C, Noll W. 2004 *The non-linear field theories of mechanics*, 3rd edn. Berlin, Germany: ringer.

encer AJMed. 1984 *Continuum theory of the mechanics of fibre-reinforced composites*, vol. 282. SM Courses and Lectures. Vienna, Austria: Springer.

50. Smith GF. 1994 *Constitutive equations for anisotropic and isotropic materials*. Amsterdam, New York, North Holland: Elsevier.
51. Spencer AJM. 1971 Theory of invariants. In *Continuum Physics*, vol. 1 (ed. AC Eringen), pp. 239–353. New York, NY: Academic Press.
52. Berdichevsky V. 2009 *Variational principles of continuum mechanics: I. Fundamentals*. Heidelberg, Germany: Springer.
53. Eremeyev VA, Rosi G, Naili S. 2016 Surface/interfacial anti-plane waves in solids with surface energy. *Mech. Res. Commun.* **74**, 8–13. (doi:10.1016/j.mechrescom.2016.02.018)
54. Parnell WJ, Norris AN, Shearer T. 2012 Employing pre-stress to generate finite cloaks for antiplane elastic waves. *Appl. Phys. Lett.* **100**, 171907. (doi:10.1063/1.4704566)
55. Achenbach J. 1973 *Wave propagation in elastic solids*. Amsterdam, The Netherlands: North Holland.
56. Eremeyev VA. 2017 On nonlocal surface elasticity and propagation of surface anti-plane waves. In *Mechanics for Materials and Technologies* (eds H Altenbach, RV Goldstein, E Murashkin), pp. 153–162. Cham, Switzerland: Springer International Publishing.
57. Steigmann DJ. 2015 Mechanical response of fabric sheets to three-dimensional bending, twisting, and stretching. *Acta Mech. Sin.* **31**, 373–382. (doi:10.1007/s10409-015-0413-x)
58. Giorgio I, Steigmann DJ. 2018 Axisymmetric deformations of a 2nd grade elastic cylinder. *Mech. Res. Commun.* **94**, 45–48. (doi:10.1016/j.mechrescom.2018.09.004)
59. Steigmann DJ. 2018 Equilibrium of elastic lattice shells. *J. Eng. Math.* **109**, 47–61. (doi:10.1007/s10665-017-9905-y)
60. Slepyan LI. 1981 Dynamics of a crack in a lattice. *Soviet Phys. Doklady* **26**, 538–540.
61. Slepyan LI. 2010 Dynamic crack growth under Rayleigh wave. *J. Mech. Phys. Solids* **58**, 636–655. (doi:10.1016/j.jmps.2010.03.003)